Computational Materials Science 87 (2014) 241–247

Contents lists available at ScienceDirect

Computational Materials Science

journal homepage: www.elsevier.com/locate/commatsci

Study the effect of martensite banding on the failure initiation in dual-phase steel

A. Ramazani [a,*], Z. Ebrahimi [b], U. Prahl [c]

[a] Department of Materials Science and Engineering, University of Michigan, 2300 Hayward St., Ann Arbor, MI 48109, USA
[b] Department of Mechanical Engineering, Payame Noor University, PO BOX 19395–3697 Tehran, Iran
[c] Department of Ferrous Metallurgy, RWTH Aachen University, Intzestr. 1, D-52072, Aachen, Germany

ARTICLE INFO

Article history:
Received 23 August 2013
Received in revised form 25 January 2014
Accepted 28 January 2014
Available online 13 March 2014

Keywords:
Dual–phase (DP) steel
Digital image correlation (DIC)
In situ bending test
EBSD
Representative volume element (RVE)
Extended finite element method (XFEM)

ABSTRACT

This work aims to study the effect of martensite banding on the failure initiation in dual-phase (DP) steel. A microstructure based approach using representative volume elements (RVE) is utilized to evaluate the microstructure deformation and the failure initiation on the mesoscale. Mini tensile test with digital image correlation (DIC) analysis was carried out and linked to local scanning electron microscopy (SEM) analysis to identify macroscopic failure initiation strain values. In situ analysis of bending test in SEM combined with electron backscatter diffraction (EBSD) measurements before and after the test showed that crack initiation occurs in martensite islands. Representative volume element (RVE) modeling combined with extended finite element method (XFEM) was applied to simulate martensite cracking on mesoscale. XFEM failure parameters have been identified based on local and macroscopic mini tensile evaluation applying classical *J*-Integral theory. The identified parameters were validated by comparing the predictions with the experimental results.

1. Introduction

Dual-phase (DP) steel is characterized by a microstructure consisting of hard martensite particles dispersed in a soft and ductile ferrite matrix. Due to this morphology, DP steels show a good combination of strength and ductility so that they are demanded extensively for the automotive industry [1–3].

Based on several researchers' reports dual-phase steels fail in a ductile manner [4–9]. These research works have described that the void initiation takes place around or inside martensite grains. Afterward, growth and coalescence of voids occurs due to ferrite failure. Speich and Miller [4] have reported that at high V_m they observed martensite cracking as main failure mechanism. Kim and Thomas [5] have reported that the formation of voids in dual-phase steels depends on the morphology of the martensite. Maire et al. [8] observed both martensite cracking and ferrite/martensite interface debonding during in situ tensile tests with three dimensional X-ray tomography. Calcagnotto et al. [9] investigated failure behavior of DP steels with different grain sizes using mini tensile test with DIC technique and showed that while in classical DP steels (of coarse grain and high impurity) the cleavage fracture and grain split cause failure, in modern DP steels (of fine grain and low impurity) grain boundaries play the significant role.

Recently, failure modeling in DP steels is a subject of interest for several research groups [10–16]. They approach the topic through different scientific methods. Ramazani et al. [10] have studied the failure of DP steels macroscopically using Gurson–Tvergaard–needleman (GTN) model. Luo and Wierzbicki [11] have investigated the failure behavior of DP steel sheet during stretch-bending operations using Mohr–Coulomb (MMC) ductile fracture criterion. Sun et al. [12] and Choi et al. [13] studied the failure mode and ultimate ductility of DP steels using a microstructure-based model at different loading and boundary conditions. Uthaisangsuk et al. [14] investigated the failure of DP steels using RVE approach. They utilized a cohesive zone and GTN models to study the ferrite–martensite debonding and ferrite degradation, respectively. Vajragupta et al. [15] and Ramazani et al. [16,17] have investigated the failure behavior of DP steel using XFEM. This research work aims to investigate the effect of martensite banding on the failure initiation behavior in DP steel utilizing XFEM.

2. Experimental procedure

Equiaxed and banded DP microstructures were processed through laboratory heat treatment from a DP600 steel composition that was delivered in a cold-rolled, ferrite–pearlite state with a

* Corresponding author. Tel.: +1 734 615 8815; fax: +1 734 763 4788.
E-mail address: ramazani@umich.edu (A. Ramazani).

http://dx.doi.org/10.1016/j.commatsci.2014.01.051
0927-0256/

Table 1
Chemical composition of the investigated DP steels (in wt%).

C	Si	Mn	P	S	Cr	Ni	Al	Cu	V
0.078	0.25	1.58	0.015	0.001	0.055	0.024	0.032	0.010	0.011

thickness of 1 mm using a Trebel hot deformation simulator [18]. Table 1 shows the chemical composition. To obtain the same percentage of martensite at different heating rates, 790 °C and 760 °C were chosen as temperatures and heating rates of 1 °C/s and 100 °C/s, respectively, were used. After annealing, the samples were quickly gas-quenched at a rate of 80 °C/s to form martensite from austenite. Different annealing temperatures were chosen in order to get the same percent of martensite in both microstructures. Eventually, martensite phase fraction was identified based on metallography as 35% in both cases.

To quantify the distribution of martensite in the laboratory-produced DP steel, three parameters were taken into account: the average height, the average length, and the aspect ratio (length-to-height ratio) of martensite islands in DP microstructures. Digimizer software was used for this purpose, and the analysis was performed automatically [19]. For an aspect ratio close to 1, the microstructure was described as an equiaxed microstructure. This was obtained at a slow heating rate of 1 °C/s, while at a fast heating rate of 100 °C/s, a banded microstructure was obtained. The aspect ratio of martensite bands was 7.2 for this particular heating rate. The ferrite grain size was respectively quantified as 5.6 and 6.1 μm for equiaxed and banded microstructures through the linear intercept method (ASTM Standard E 112). Using Thermocalc TCFE6.7 according to the approach as described in [20], carbon content in ferrite and martensite was calculated as 0.0035% and 0.216% for equiaxed microstructure and as 0.0045% and 0.214% for banded microstructure, respectively.

In order to identify the crack initiation and the correspondent local strain, three parallel mini tensile tests with digital image correlation (DIC) technique were carried out parallel to the rolling direction [21]. The geometry and dimensions of tensile test specimen are illustrated in Fig. 1(a). During the tests, images were taken from the surface in every second. So, strain distributions can be captured in different deformation steps in the evaluated zone. SEM Analysis was performed to observe the microstructure of the material in the center line along loading direction in order to observe where the crack initiates and to identify the responsible strain (Fig. 1(b)) [16,17].

In order to identify the failure initiation mechanism and to validate the failure initiation modeling in situ three point bending test with EBSD measurement before and after the test was carried out at room temperature on the DP steel specimen with equiaxed microstructure using a 5000 N/800 °C bending module by Kammrath & Weiss. The test procedure and the sample geometry are schematically shown in Fig. 2. Rolling direction was considered parallel to the major stress direction. On a strip of 11 mm × 60 mm

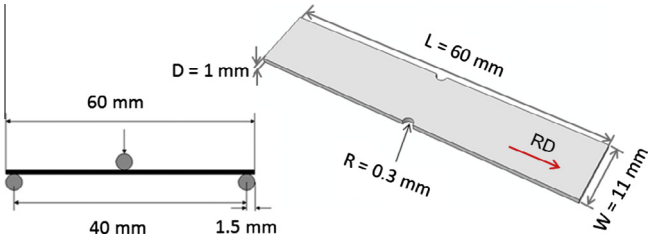

Fig. 2. Bending test procedure and sample geometry for LC-SEM in situ bending test.

with a thickness of 1 mm, a three-point bending test was performed. In order to better localize the area of probable crack formation, the strip was notched at the sides at the position close to the central rod of the bending device. During the bending tests, the applied force was increased incrementally.

However, the load was held stepwise after a specified deformation in order to record the surface images of the samples in the LC-SEM. The LC-SEM was adjusted to obtain an SEM image focusing on the area between two pre-existing notches in both sides in order to catch the process of crack initiation at the surface while displacement-controlled load was applied to the samples. The LC-SEM analysis was made on the surface at the tensile loaded side of the bended specimen as the loads will be highest here. During loading, displacement and load were recorded automatically. Additionally, SEM images were taken at any moments when changes in mesoscale structure or damage growth occurred on the specimen's surface.

Hence, the mechanical loading causing the microcrack formation could be identified precisely and it can be identified where the crack starts in the microstructure. Additionally, EBSD measurements were made before and after the test in the same surface area in order to identify whether martensite or ferrite/martensite interface fails first. Finally, IQ, IPF map and Kernel average misorientation map before and after the in situ test were compared with micromechanical failure simulation in order to validate the modeling approach.

3. Micromechanical modeling

In a former study, the acceptable size of the RVE was considered as a minimum of 24 μm while it should include at least 19 martensite particles [19]. A 2D RVE from SEM images was developed using an in-house program (see Fig. 3). Quadratic elements with the size of 0.25 μm were used. Periodic boundary conditions were imposed on the RVE. The elastic modulus for ferrite and martensite is assumed to be 210 GPa. The flow curve of individual phases for ferrite and martensite is quantified based on a dislocation density based strain hardening model. The full approach has been given in a former study [20,22].

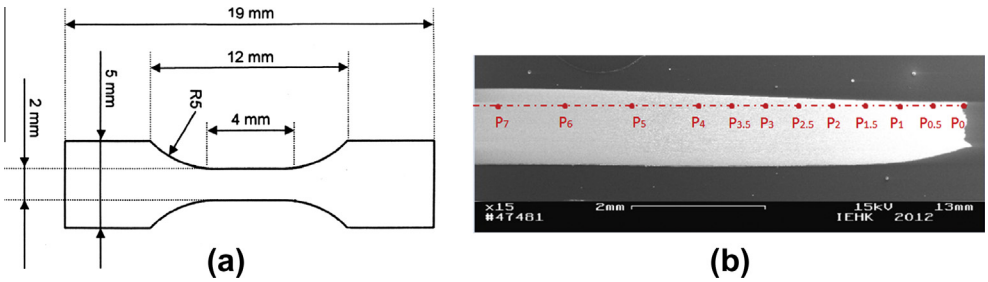

Fig. 1. (a) Geometry and dimensions of the mini geometry in situ tensile test specimens and (b) positions of SEM analysis in center line of broken specimen.